

Slow sound in matter-wave dark soliton arrays

Muzzamal I. Shaukat,^{1,2} Eduardo V. Castro,^{1,3} and Hugo Terças⁴

¹*CeFEMA, Instituto Superior Técnico, Universidade de Lisboa, Lisboa, Portugal*

²*University of Engineering and Technology, Lahore (RCET Campus), Pakistan**

³*Centro de Física das Universidades do Minho e Porto, Departamento de Física e Astronomia, Faculdade de Ciências, Universidade do Porto, Porto, Portugal*

⁴*Instituto de Plasmas e Fusão Nuclear, Lisboa, Portugal†*

We show the existence of slow propagating phonons in quasi one dimensional Bose-Einstein condensates. The impurities are trapped inside the potential created by dark-soliton due to which the conditions to separate the three levels (qutrit), perfectly, has determined. We compute the phonon-soliton coupling and investigate the decay rates of the three level system. We derive the analytical expression of the linear susceptibility to demonstrate the phenomenon of acoustic induced transparency based on matter wave phononics. The dark-soliton qutrit with unique properties of transmission and dispersion revealing the possibility of slowing down the speed of acoustic pulse. Moreover, the present scheme could be proposed to analyze the diverse applications like quantum gates in the field of quantum information.

PACS numbers: 67.85.Hj 42.50.Lc 42.50.-p 42.50.Md

Introduction. Electromagnetically induced transparency (EIT) [1] is a quantum interference effect in which the absorption of a weak probe laser, interacting resonantly with an atomic transition, is reduced in the presence of a coupling laser. EIT is, for instance, crucial in optically controlled slowing of light [2] and optical storage [3], having been extensively investigated in Λ , V and cascade-type three-level atoms [4, 5], and experimentally observed in atoms [6] and semiconductor quantum wells [7]. A major problem in the initial studies of EIT in atomic vapors has to do with the thermal spectral broadening [8, 9], smearing out the EIT window. In order to mitigate this issue, researchers have made use of highly coherent BECs [10–12]. The association of EIT with light-matter coupling can be used to prepare and detect coherent many-body phenomena in ultra-cold quantum gases [13].

Soon after the engineering of photonic crystal structures, the attention has been drawn to the propagation of acoustic waves in periodic media [14, 15]. Many intriguing phenomena, such as the analogue of EIT [16, 17] and Fano resonances [18, 19] have been envisaged in the context of acoustics as well [20, 21]. For example, an isotropic metamaterial consisting of grooves on a square bar traps enhances the acoustic waves due to a strong modulation of wave group velocity [22]; slowing down the speed of sound in sonic crystal waveguides has also been achieved, with a reported group velocity of 26.7 m/s [23]. Soliton propagation and soliton-soliton interaction in EIT media has been studied by Wadati et al. [24], and the formation of solitons via dark-state polaritons has been proposed [25].

Recently, we have shown that a dark-soliton (DS) qubit in a quasi one dimensional (1D) BEC are appealing candidates to store information given their appreciably long lifetimes ($\sim 0.01 - 1$ s) [26]. Moreover, we explored the

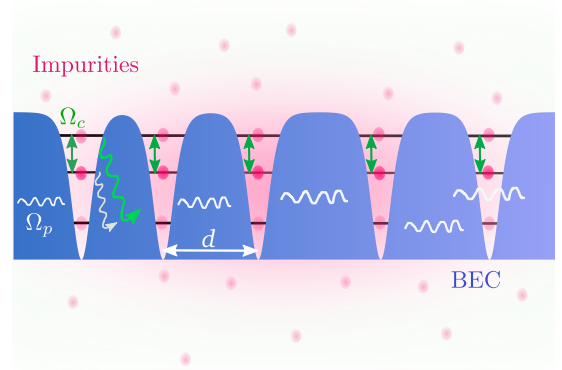


FIG. 1: (color online) Schematic representation of dark soliton qutrit immersed in a BEC. The impurities (free particles) considered dark soliton as potential. Wiggly lines shows the quantum fluctuations (phonons).

creation of entanglement between DS qubits, at appreciable large distances of the order of few micrometer, by using the superposition of two maximally entangled states in the dissipative process of spontaneous emission [27, 28]. Dark-soliton qubits thus offer an appealing alternative to quantum optics in solid-state platforms, where information processing involves only phononic degrees of freedom: the quantum excitations on top of the BEC state.

In this Letter, we propose to make use of dark-soliton to achieve a phenomenon with EIT-like characteristics, the *acoustic transparency* (AT). The active medium is composed of a set of dark-soliton *qutrits*, i.e. three-level object comprising an impurity trapped at the interior of a dark-soliton potential, in which the BEC acoustic modes propagate (see Fig. 1 for a schematic representation). We start by recalling the conditions under which that qutrit is possible. The qutrit array is shown to be

an open quantum system, where the reservoir is determined by quantum fluctuations (phonons) on top of the BEC state [29]. We compute the linewidth of each of the qutrit transitions by treating the qutrit-phonon interaction within the Born-Markov approximation and analyze the dependence of absorption profile of the AT on the BEC-impurity coupling. We conclude by computing the dispersion relation of a weak envelope of sound waves and show that it propagates at very low speeds (~ 0.06) mm/s, to the best of our knowledge a record value in acoustics. Our study represents an advance in the direction of ‘slow-sound’ schemes and the results have potential applications in phononic information processing.

Dark-soliton qutrit. We start by considering a dark soliton in a quasi 1D BEC, with the later being surrounded by a dilute gas of impurities (see Fig. 1). The DS plays the role of a potential for the impurities (considered to be free particles) and the quantum fluctuations (phonons) act like a proper reservoir. At the mean field level, the system is governed by the Gross-Pitaevskii and Schrödinger equations,

$$\begin{aligned} i\hbar \frac{\partial \psi_1}{\partial t} &= -\frac{\hbar^2}{2m_1} \frac{\partial^2 \psi_1}{\partial x^2} + g_{11} |\psi_1|^2 \psi_1 + g_{12} |\psi_2|^2 \psi_1, \\ i\hbar \frac{\partial \psi_2}{\partial t} &= -\frac{\hbar^2}{2m_2} \frac{\partial^2 \psi_2}{\partial x^2} + g_{21} |\psi_{\text{sol}}|^2 \psi_2, \end{aligned} \quad (1)$$

where g_{11} represents the BEC inter-particle interaction strength, $g_{12} = g_{21}$ is the BEC-impurity coupling constant [30] and m_1, m_2 denotes the BEC particle and impurity masses, respectively. The singular nonlinear solution corresponding to the soliton profile is $\psi_{\text{sol}}(x) = \sqrt{n_0} \tanh[x/\xi]$ [31, 32], where n_0 denotes the BEC linear density, $\xi = \hbar/\sqrt{m_1 n_0 g}$ is the healing length (of the order (0.7 – 1.0) μm , respectively, in a typical 1D BECs, for which the condensate is homogeneous along a trap of size $l_z \sim 70 \mu\text{m}$ [33]). More recent experiments leads eventual trap inhomogeneities to be much less critical by creating much larger traps, $l_z \sim 100 \mu\text{m}$ [34]. Therefore, Eq. (1) can be written as

$$E' \psi_2 = -\frac{\hbar^2}{2m_2} \frac{\partial^2 \psi_2}{\partial x^2} - g_{21} n_0 \text{sech}^2\left(\frac{x}{\xi}\right) \psi_2, \quad (2)$$

where $E' = E - n_0 g_{21}$. Notice that these results can be easily generalised for the case of gray soliton (travelling with speed v) by replacing $\psi_{\text{sol}}(x) = \sqrt{n_0} [i\theta + \gamma \tanh[x\gamma/\xi]]$, where $\theta = v/c_s$ and $\gamma = (1 - \theta^2)^{1/2}$. To find the analytical solution of Eq. (2), the potential is casted in the form $V(x) = -\hbar^2 \nu(1 + \nu) \text{sech}^2(x/\xi)/2m_2 \xi^2$ [3] with $2\nu = -1 + \sqrt{1 + 4g_{21}m_2/g_{11}m_1}$ and the energy spectrum $E'_n = -\hbar^2(\nu - n)^2/2m_2 \xi^2$, where n is an integer [30]. The number of bound states created by the DS is $n_{\text{bound}} = \lfloor \nu + 1 + \sqrt{\nu(1 + \nu)} \rfloor$, where the symbol $\lfloor \cdot \rfloor$ denotes the integer part. As such, for a DS to contain exactly three

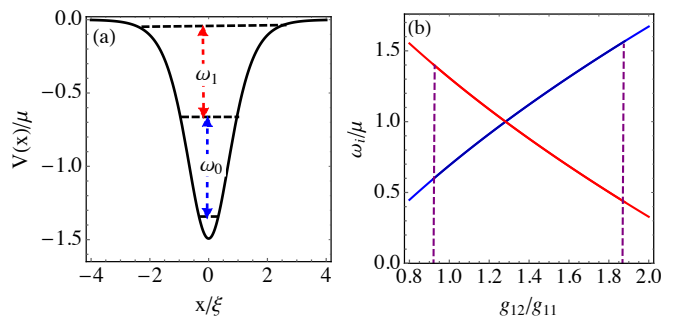


FIG. 2: (color online) Panel (a) illustrates the dark-soliton states where ω_i ($i = 0, 1$) determines the transition frequency of respective states. Panel (b) shows the dependence of transition frequency ω_i on the BEC-impurity coupling g_{12} . The vertical dashed lines corresponds to the range $4/5 \leq \nu < 9/7$ defined for the qutrit.

bound states (i.e. the condition for the qutrit to exist), the parameter ν must lie in the range

$$\frac{4}{5} \leq \nu < \frac{9}{7}. \quad (3)$$

At $\nu \geq 9/7$, the number of bound states increases. However, the effect of the impurity on the profile of the soliton itself becomes more important, and therefore special care must be taken in the choices of the mass ratio m_2/m_1 [30].

Quantum fluctuations. The total BEC quantum field includes the DS wave function and quantum fluctuations, $\psi_1(x) = \psi_{\text{sol}}(x) + \delta\psi(x)$, where $\delta\psi(x) = \sum_k (u_k(x)b_k + v_k^*(x)b_k^\dagger)$ and b_k are the bosonic operators verifying the commutation relation $[b_k, b_q^\dagger] = \delta_{k,q}$. The amplitudes $u_k(x)$ and $v_k(x)$ satisfy the normalization condition $|u_k(x)|^2 - |v_k(x)|^2 = 1$ and are explicitly given in [30]. The total Hamiltonian then reads $H = H_q + H_p + H_{\text{int}}$, where $H_q = \hbar\omega_{e_2}|e_2\rangle\langle e_2| + \hbar\omega_{e_1}|e_1\rangle\langle e_1| + \hbar\omega_g|g\rangle\langle g|$ is the qubit Hamiltonian, with $\omega_1 = \hbar(2\nu - 3)/(2m\xi^2)$ and $\omega_0 = \hbar(2\nu - 1)/(2m\xi^2)$ are the gap energies for $|e_2\rangle \rightarrow |e_1\rangle$ and $|e_1\rangle \rightarrow |g\rangle$ transitions, respectively. The term $H_p = \sum_k \epsilon_k b_k^\dagger b_k$ represents the phonon (reservoir) Hamiltonian, where $\epsilon_k = \mu\xi\sqrt{k^2(\xi^2 k^2 + 2)}$ is the Bogoliubov spectrum with chemical potential $\mu = gn_0$. The interaction Hamiltonian is given by

$$H_{\text{int}} = g_{12} \int dx \psi_2^\dagger \psi_1^\dagger \psi_1 \psi_2, \quad (4)$$

where $\psi_2(x) = \sum_{l=0}^2 \varphi_l(x)a_l$ describes the qutrit wave function in terms of the bosonic operators a_n , with $\varphi_0(x) = A_0 \text{sech}^\alpha(x/\xi)$, $\varphi_1(x) = 2A_1 \tanh(x/\xi)\varphi_0(x)$ and $\varphi_2(x) = \sqrt{2}A_2(1 - (1 + 2\alpha)\tanh^2(x/\xi))\varphi_0(x)$, where A_j ($j = 0, 1, 2$) are the normalization constants and $\alpha = \sqrt{2g_{12}m_2/g_{11}m_1}$ [30]. Using the rotating wave approximation (RWA), the first order perturbed Hamiltonian

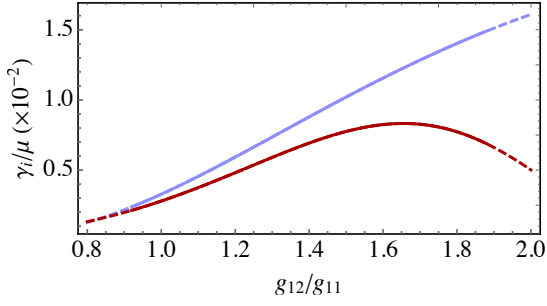


FIG. 3: (color online) Dependence of the decay rates γ_0 (blue line) and γ_1 (red line) on the BEC-impurity coupling. The solid lines correspond to the range $\frac{4}{5} \leq \nu < \frac{9}{7}$ that defines the qutrit. We have used $m_2 = 1.56m_1$, corresponding to a ^{133}Cs impurity loaded in a ^{133}Rb BEC dark soliton.

can be written as

$$H_{\text{int}}^{(1)} = \sum_k (g_0^k \sigma_0^+ + g_1^k \sigma_1^+) b_k + (g_0^{k*} \sigma_0^- + g_1^{k*} \sigma_1^-) b_k^\dagger, \quad (5)$$

where $\sigma_{0,1}^+ = a_{e_1, e_2}^\dagger a_{g, e_1}$, $\sigma_{0,1}^- = a_{g, e_1}^\dagger a_{e_1, e_2}$ and the coupling constants $g_{i\mu}^k = g_i^k (i = 0, 1)$ are explicitly given in [30]. In our RWA calculation, the counter-rotating terms proportional to $b_k \sigma_i^-$ and $b_k^\dagger \sigma_i^+$ are dropped. The accuracy of such an approximation can be verified *a posteriori*, provided that the emission rates γ_0 and γ_1 are much smaller than the qutrit transition frequencies ω_0 and ω_1 , respectively.

Wigner-Weisskopf spontaneous decay. We employ the Wigner-Weisskopf theory to find the spontaneous decay rate of the states, by neglecting the effect of temperature and other external perturbations [36]. In this regard, the qutrit is assumed to be initially at the excited state $|e_2\rangle$ and the phonons to be in the vacuum state $|0\rangle$. Under such conditions, the wave function of total system (qutrit + phonons) can be described as

$$|\phi(t)\rangle = a(t) |e_2, 0\rangle + \sum_k b_k(t) |e_1, 1_k\rangle + \sum_{k,p} b_{k,p}(t) |g, 1_k, 1_p\rangle, \quad (6)$$

where $a(t)$ is the probability amplitude of the excited state $|e_2\rangle$. The qutrit decays to the state $|e_1\rangle$ with probability amplitude $b_k(t)$ by emitting a phonon of wavevector k and frequency ω_k . Subsequently, the qutrit de-excites to the ground state $|g\rangle$ via the emission of p -phonon of frequency ω_p and probability amplitude $b_{k,p}(t)$. In the interaction picture, these coefficients can be written as [30],

$$a(t) = e^{-\gamma_1 t/2},$$

$$b_k(t) = -i g_0^k \frac{[e^{i(\omega_k - \omega_1)t - \gamma_1 t/2} - e^{-\gamma_0 t/2}]}{i(\omega_k - \omega_1) - \frac{\gamma_1 - \gamma_0}{2}},$$

$$b_{k,p}(t) = \frac{g_0^k g_1^k}{i(\omega_k - \omega_1) - \frac{\gamma_1 - \gamma_0}{2}} \left[\frac{e^{i(\omega_p - \omega_0)t - \gamma_0 t/2} - 1}{i(\omega_p - \omega_0) - \frac{\gamma_0}{2}} + \frac{1 - e^{i(\omega_k + \omega_p - \omega_{eg})t - \gamma_1 t/2}}{i(\omega_k + \omega_p - \omega_{eg}) - \frac{\gamma_1}{2}} \right], \quad (7)$$

where $\omega_{eg} = \omega_0 + \omega_1$ and γ_i ($i = 0, 1$) is the i th state decay rate

$$\gamma_i = \frac{L}{\sqrt{2}\hbar\xi} \int d\omega_k \frac{\sqrt{1 + \eta_i}}{\eta_i} |g_i^k|^2 \delta(\omega_k - \omega_i), \quad (8)$$

where $\eta_i = \sqrt{\mu^2 + \hbar^2 \omega_i^2}$. Both RWA and Born-Markov approximations can be verified from Fig. 7 and Fig. 3, where it is depicted that the decays rates of both the transitions are much smaller than the respective transition frequencies. It is pertinent to mention here that Feshbach resonances can be used to tune the value of g_{12} experimentally, allowing for an additional control of the rates γ_i . Moreover, dark-soliton quantum diffusion may be the only immediate limitation to the performance of this proposal [4], a feature that has been theoretically predicted but yet not experimentally validated. In any case, quantum evaporation is expected if important trap anisotropies are present, a limitation that we can overcome with the help of box-like or ring potentials [33].

Acoustic Bloch equations. To analyze the interference effect of AT, we consider the situation where the qutrit is externally driven by two (probe and control) acoustic fields. The probe field can be excited with a Raman Laser driving the transition $|g\rangle \leftrightarrow |e_1\rangle$ with frequency ω_p and detuning $\Delta_p = \omega_p - \omega_0$. Simultaneously, a Raman laser field of frequency ω_c and detuning $\Delta_c = \omega_c - \omega_1$ couple the states $|e_1\rangle$ and $|e_2\rangle$ [38]. Therefore, the qutrit driving can be described, within the RWA approximation, by the following Hamiltonian

$$H_{\text{drive}} = \frac{\hbar}{2} (\Omega_p |e_1\rangle \langle g| + \Omega_c |e_2\rangle \langle e_1| - 2\Delta_p |e_1\rangle \langle e_1| - 2\delta |e_2\rangle \langle e_2|) + \text{H.c.}, \quad (9)$$

where $\delta = \Delta_p + \Delta_c$ and $\Omega_{p,c}$ denote the Rabi frequency of the probe and control fields, respectively. We obtain the solution for the density matrix ρ by solving the master equation

$$\dot{\rho}_q(t) = -\frac{i}{\hbar} [H_q, \rho_q(t)] + \sum_{i=0}^1 \gamma_i \mathcal{L}_i[\rho], \quad (10)$$

with $\rho_{ij} = \rho_{ji}^*$ and the Lindblad operator $\mathcal{L}[\rho] = [\sigma_- \rho_q(t) \sigma_+ - \frac{1}{2} \{\sigma_+ \sigma_-, \rho_q(t)\}]$. In the limit of the weak-probe approximation, $\Omega_p \ll \Omega_c$, the steady state-coherences are given by

$$\rho_{21} = \frac{i\Omega_p}{(\gamma_0 - 2i\Delta_p) + \frac{\Omega_c^2}{\gamma_1 - 2i\delta}},$$

$$\rho_{31} = \frac{-i\Omega_c}{(\gamma_1 - 2i\delta)} \rho_{21}. \quad (11)$$

In what follows, we assume that a set of solitons (i.e. a soliton gas [39]) of density $N = 1/d$, with d denoting the average distance between the solitons. If the solitons are well-separated, $d \ll \xi$, we can assume the qutrits to be independent. This is not usually the case in one-dimensional systems, unless in the especial comensurability situation, as a consequence of the infinite-range (sinusoidal) character of the collective decay rate [40, 41]. Fortunately in our case, because the solitons locally deplete the BEC, the collective scattering rate vanishes at distances largely exciding the healing length, $d \gg \xi$ [27, 28]. As such, we can determine the long wavelength behaviour, $kd \ll 1$, of the probe field envelope. Using the Heisenberg's relation $i\hbar\partial(\delta\Psi)/\partial t = [\hat{H}, \delta\Psi]$ and the fluctuating field $\delta\Psi = \phi b_q e^{iqx} + \psi^* b_q^\dagger e^{-iqx}$, where ϕ and ψ are the Bogoliubov coefficients, we obtained the propagating equation [30]

$$\frac{\partial\Omega_p}{\partial t} + \frac{\omega_q}{q} \frac{\partial\Omega_p}{\partial x} = -\frac{i}{2\hbar^2}(g_0^k)^2 \rho_{12}, \quad (12)$$

where $\Omega_p = g_0^{k_{\text{res}}} \delta\Psi/\hbar$, $k_{\text{res}} = 0.9/\xi$ is the resonant wavevector. By ignoring the time derivative from Eq. (33) (time-independent fluctuating field) and comparing it with $\partial_z \delta\Psi = ik\chi \delta\Psi/2$ [42], we express the susceptibility

$$\chi = -\frac{iN\xi(g_0^{k_{\text{res}}})^2}{\hbar\epsilon_k\{(\gamma_0 - 2i\Delta_p) + \frac{\Omega_c^2}{\gamma_1 - 2i\delta}\}}, \quad (13)$$

where $\rho_{12}^{\text{gas}} = N\xi\rho_{12}$ with the total number of solitons per unit length N in the system and the size of the soliton ξ . The acoustic response of the envelope can be determined by the refractive index $n = \sqrt{1 + \chi}$. The onset of the AT is demonstrated in Fig. 4. The system reveals initially a normal Lorentzian peak under $\Omega_c \ll \gamma_1$ but a dip immediately appears as we increase the control laser power Ω_c . Moreover, the width of the transparency window increases significantly for $\Omega_c \gg \gamma_1$, and carries a signature of Autler-Townes doublet. We expect that the destructive interference between the excitation pathways is reduced due to large value of γ_1 . It is important to realize that a change in absorption over a narrow spectral range must be accompanied by a rapid and positive change in refractive index due to which a very low group velocity is produced in AT. Therefore, the group velocity for the acoustic field is given by

$$v_g = \frac{c_s}{1 + \frac{\chi_R}{2} + \frac{\omega_p}{2}(\partial\chi_R/\partial\omega_p)}, \quad (14)$$

where we assume that $\Omega_c^2 \gg \Gamma_p\Gamma_c$.

Slow sound in box potentials.—For the sake of experimental estimates, we consider a one-dimensional BEC loaded in a large box potential. In a typical trap of size $\sim 100 \mu\text{m}$, healing length $\xi \sim 0.7 \mu\text{m}$ and sound speed

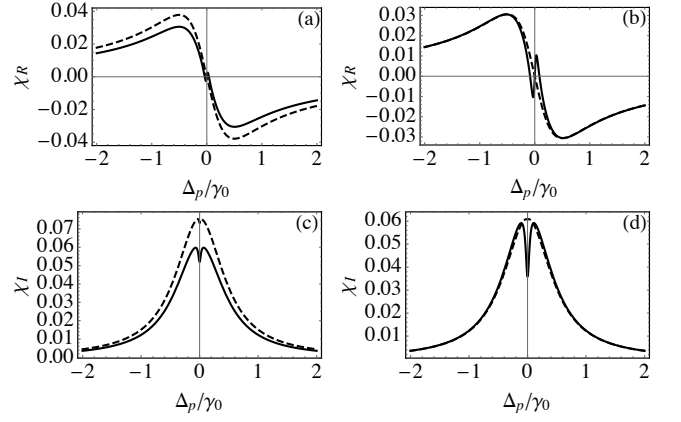


FIG. 4: (color online) Acoustic susceptibility χ dependence on the probe detuning Δ_p . Left panel depicts the (a) dispersion and (c) absorption spectra for BEC-Impurity coupling $g_{12} = 1.1g_{11}$ (dashed line) and $g_{12} = 1.85g_{11}$ (solid line), where $\Omega_c > \gamma_1$. AT effects diminishes gradually at smaller g_{12} but as we increase coupling g_{12} , we observe AT effects. Right panel illustrates the (b) dispersion and (d) absorption for $\Omega_c = 0.2\gamma_0$ (dashed line) and $\Omega_c = 2\gamma_0$ (solid line). The transparency widens and the dispersion becomes steeper only when $\Omega_c \gg \gamma_1$.

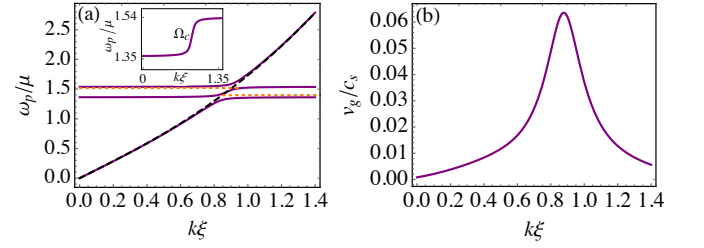


FIG. 5: (color online) Panel (a) depicts the dispersion curve, where the solid line illustrates the solution of Eq. (12) for $g_{12} = 1.85g_{11}$ and dashed line shows the Bogoliubov energy spectrum. The inset shows the dependence of absorption (transparency) width on the coupled frequency Ω_c . Panel (b) determines the group velocity v_g of the order of 0.06 of the sound speed c_s . In all cases, we have set $m_2 = 1.56m_1$ and a soliton concentration of $N\xi = 0.2$.

$c_s \sim 1 \text{ mm/s}$ [33], we can imagine placing up to 20 well-separated ($d \sim 3.5 \mu\text{m}$) solitons. Under these conditions, the envelope group velocity can be brought down to a record value of $\sim 0.06 \text{ mm/s}$, corresponding to the peak appearing in Fig. 5. Indeed, for a wavelength compared to a intersoliton separation d , the estimated group velocity is $v_g \simeq 5.0 \mu\text{m/s}$. The latter is much smaller than obtained in band-gap arrays [43] and detuned acoustic resonators [44]. In the latter, a sound speed of $\sim 9.8 \text{ m/s}$ is experimentally reported, which makes our scheme able to achieve a 10^{-5} smaller speed for an acoustic pulse.

In conclusion, we proposed a scheme for the realization of the acoustic transparency phenomenon with dark-solitons qutrits in a quasi-one dimensional Bose-Einstein

condensates. The qutrits consist of three-level structures formed by impurities trapped by the dark solitons. We investigate the spontaneous decay rates to analyze the interference effect of the acoustic transparency, due to which a narrow absorption window, depending on the BEC-impurity coupling, can be achieved. We show that an acoustic pulse can be slowed down to a record speed of 0.06 mm/s. We believe that the suggested approach opens a promising research avenue in the field of acoustic transport. In general, the present scheme will provide a great feasibility to enable the numerous applications like quantum gates in the field of quantum information processing [45, 46].

The authors acknowledge the support from the DP-PMI programme and Fundação para a Ciência e a Tecnologia (Portugal), namely through the grants No. SFRH/PD/BD/113650/2015 and IF/00433/2015. E.V.C. and M.I.S acknowledge partial support from FCT-Portugal through Grant No. UID/CTM/04540/2013.

* Electronic address: muzzamalshaukat@gmail.com

† Electronic address: hugo.tercas@tecnico.ulisboa.pt

- [1] S. E. Harris, J. E. Field and A. Imamoglu, Phys. Rev. Lett. **64**, 1107 (1990).
- [2] L. V. Hau, S. E. Harris, Z. Dutton, and C. H. Behroozi, Nature (London) **397**, 594 (1999).
- [3] D. F. Phillips, A. Fleischhauer, A. Mair, R. L. Walsworth, and M. D. Lukin, Phys. Rev. Lett. **86**, 783 (2001).
- [4] T. Y. Abi-Salloum, Phys. Rev. A **81**, 053836 (2010).
- [5] P. M. Anisimov, J. P. Dowling and B. C. Sanders, Phys. Rev. Lett. **107**, 163604 (2011).
- [6] K. J. Boller, A. Imamoglu and S. E. Harris, Phys. Rev. Lett. **66**, 2593 (1990).
- [7] G. B. Serapiglia, E. Paspalakis, C. Sirtori, K. L. Vodopyanov and C. C. Philips, Phys. Rev. Lett. **84**, 1019 (2000).
- [8] E. A. Cornell and C. E. Wieman, Rev. Mod. Phys. **74**, 875 (2002).
- [9] W. Ketterle, Rev. Mod. Phys. **74**, 1131 (2002).
- [10] I. Vadeiko, A. V. Prokhorov, A. V. Rybin, and S. M. Arakelyan, Phys. Rev. A **72** 013804 (2005).
- [11] J. G. Ri, C. K. Kim and K. Nahm, Commun. Theor. Phys. **48**, 461464 (2007).
- [12] V. Ahufinger, R. Corbalan, F. Cataliotti, S. Burger, F. Minardi, and C. Fort, Opt. Comm. **211**, 159 (2002).
- [13] J. Ruostekoski, and D. F. Walls, Phys. Rev. A **59**, R2571 (1999).; *ibid* Eur. Phys. J. D **5**, 335 (1999).
- [14] E. Lheurette, *Metamaterials and Wave Control* (Wiley-ISTE, London) (2013).
- [15] R. V. Craster and S. Guenneau, *Acoustic Metamaterials: Negative Refraction, Imaging, Lensing and Cloaking* (Springer, Berlin), Vol. 166 (2013).
- [16] N. Liu, L. Langguth, T. Weiss, J. Kastel, M. Fleischhauer, T. Pfau, and H. Giessen, Nat. Mater. **8**, 7587762 (2009).
- [17] M. Fleischhauer, A. Imamoglu, and J. P. Marangos, Rev. Mod. Phys. **77**, 633 (2005).
- [18] B. Lukyanchuk, N. I. Zheludev, S. A. Maier, N. J. Halas, P. Nordlander, H. Giessen, and C. T. Chong, Nat. Mater. **9**, 7077715 (2010).
- [19] C. Wu, A. B. Khscianikaev, R. Adato, N. Arju, A. A. Yanik, H. Altug, and G. Shvets, Nat. Mater. **11**, 69775 (2011).
- [20] A. Santillan and S. I. Bozhevolnyi, Phys. Rev. B **84**, 064304 (2011).
- [21] M. Amin, A. Elayouch, M. Farhat, M. Addouche, A. Kheelif, and H. Bagci, J. App. Phys. **118**, 164901 (2015).
- [22] J. Zhu, Y. Chen, X. Zhu, F. J. Garcia-Vidal, X. Yin, W. Zhang, and X. Zhang, Sci. Rep. **3**, 1728 (2013).
- [23] A. Cicek, O. A. Kaya, M. Yilmaz, and B. Ulug, J. Appl. Phys. **111**, 013522 (2012).
- [24] M. Wadati, Eur. Phys. J. Special Topics **173**, 223 (2009).
- [25] X. J. Liu, H. Jing and M. L. Ge, Phys Rev. A **70**, 055802 (2004).
- [26] M. I. Shaukat, E. V. Castro and H. Terças, Phys. Rev. A **95**, 053618 (2017).
- [27] M. I. Shaukat, E. V. Castro and H. Terças, [arXiv:1801.08169](https://arxiv.org/abs/1801.08169) (2018).
- [28] M. I. Shaukat, E. V. Castro and H. Terças, [arXiv:1801.08894](https://arxiv.org/abs/1801.08894) (2018).
- [29] L. Pitaevskii and S. Stringari, *Bose-Einstein Condensation*, Clarendon, Oxford (2003).
- [30] See Supplemental Material for details on the calculation of the qutrit level structure, on the rotating wave approximation performed to obtain Eq. (5), on the computation of the spontaneous decay rates and on the equation governing the probe envelope dynamics.
- [31] V. E. Zakharov and A. B. Shabat, Sov. Phys. JETP **34**, 62 (1972); *ibid* **37**, 823 (1973).
- [32] G. Huang, J. Szeftel, and S. Zhu, Phys. Rev. A **65**, 053605 (2002).
- [33] A. L. Gaunt, T. F. Schmidutz, I. Gotlibovych, R. P. Smith, and Z. Hadzibabic, Phys Rev. Lett. **110**, 200406 (2013).
- [34] P. Krüger, S. Hofferberth, I. E. Mazets, I. Lesanovsky, and J. Schmiedmayer, Phys. Rev. Lett. **105**, 265302 (2010).
- [35] J. Lekner, Am. J. Phys. **75**, 1151 (2007).
- [36] M. Scully and M. Zubairy, *Quantum Optics*, Cambridge University Press (1997).
- [37] J. Dziarmaga, Phys. Rev. A **70**, 063616 (2004).
- [38] E. Compagno, G. D. Chiara, D. G. Angelakis and G. M. Palma, Sci. Reports **7**, 2355 (2017).
- [39] H. Terças, D. D. Solnyshkov and G. Malpuech, Phys. Rev. Lett. **110**, 035302 (2013); *ibid* **113**, 036403 (2014).
- [40] A. Gonzalez-Tudela, D. Martin-Cano, E. Moreno, L. Martin-Moreno, C. Tejedor, and F. J. Garcia-Vidal, Phys. Rev. Lett. **106**, 020501 (2011).
- [41] T. Ramos, H. Pichler, A. J. Daley, P. Zoller, Phys. Rev. Lett. **113**, 237203 (2014).
- [42] P. Lambropoulos and D. Petrosyan, "Fundamentals of quantum optics and quantum information" (Berlin, Springer) (2007).
- [43] W. M. Robertson, C. Baker and C. B. Bennett, Am. J. Phys. **72**, 255 (2004).
- [44] A. Santillan and S. I. Bozhevolnyi, Phys. Rev. B **89**, 184301 (2014).
- [45] H. S. Borges and C. J. Villas-Boas, Phys. Rev. A **94**, 052337 (2016).
- [46] O. Lahad and O. Firstenberg, Phys. Rev. Lett. **119**, 113601 (2017).

SUPPLEMENTAL MATERIAL

Dark solitons in Bose-Einstein Condensates.— We consider a dark soliton in a quasi 1D BEC, which in turn is surrounded by a dilute set of impurities (see Fig. 1 of the main manuscript). The BEC and the impurity particles are described by the wave functions $\psi_1(x, t)$ and $\psi_2(x, t)$, respectively. At the mean field level, the system is governed by the Gross Pitaevskii and Schrodinger equation, respectively,

$$\begin{aligned} i\hbar \frac{\partial \psi_1}{\partial t} &= -\frac{\hbar^2}{2m_1} \frac{\partial^2 \psi_1}{\partial x^2} + g_{11} |\psi_1|^2 \psi_1 + g_{12} |\psi_2|^2 \psi_1, \\ i\hbar \frac{\partial \psi_2}{\partial t} &= -\frac{\hbar^2}{2m_2} \frac{\partial^2 \psi_2}{\partial x^2} + g_{21} |\psi_1|^2 \psi_2, \end{aligned} \quad (15)$$

Here, the discussion is restricted to repulsive interactions ($g_{11} > 0$) where the dark solitons are assumed to be not significantly disturbed by the presence of impurities, which we consider to be fermionic in order to avoid condensation at the bottom of the potential and $g_{12} = g_{21}$. To achieve this, the impurity gas is choosed to be sufficiently dilute, i.e. $|\psi_1|^2 \gg |\psi_2|^2$, and much massive than the BEC particles. Such a situation can be produced, for example, choosing ^{133}Cs impurities in a ^{85}Rb BEC [1]. Therefore, the impurities can be regarded as free particles that feel the soliton as a potential

$$i\hbar \frac{\partial \psi_2}{\partial t} = -\frac{\hbar^2}{2m} \frac{\partial^2 \psi_2}{\partial x^2} + g_{21} |\psi_{\text{sol}}|^2 \psi_2, \quad (16)$$

where the singular nonlinear solution corresponding to the soliton profile is $\psi_{\text{sol}}(x) = \sqrt{n_0} \tanh[x/\xi]$. The time-independent version of Eq. (16) reads

$$(E - g_{21}n_0)\psi_2 = -\frac{\hbar^2}{2m_2} \frac{\partial^2 \psi_2}{\partial x^2} - g_{21}n_0 \text{sech}^2\left(\frac{x}{\xi}\right) \psi_2, \quad (17)$$

To find the analytical solution of Eq. (17), the potential is casted in the Pöschl-Teller form

$$V(x) = -\frac{\hbar^2}{2m\xi^2} \nu(\nu + 1) \text{sech}^2\left(\frac{x}{\xi}\right), \quad (18)$$

with $\nu = \left(-1 + \sqrt{1 + 4g_{21}m_2/g_{11}m_1}\right)/2$. The particular case of ν being a positive integer belongs to the class of *reflectionless* potentials [3], for which an incident wave is totally transmitted. For the more general case considered here, the energy spectrum associated to the potential in Eq. (18) reads

$$E'_n = -\frac{\hbar^2}{2m\xi^2} (\nu - n)^2, \quad (19)$$

where n is an integer. The number of bound states created by the dark soliton is $n_{\text{bound}} = \lfloor \nu + 1 + \sqrt{\nu(1 + \nu)} \rfloor$, where the symbol $\lfloor \cdot \rfloor$ denotes the integer part. As such, the condition for *exactly* three bound states (i.e. the condition for the qutrit to exist) is obtained if ν sits in the range

$$\frac{4}{5} \leq \nu < \frac{9}{7}, \quad (20)$$

as discussed in the manuscript. At $\nu \geq 9/7$, the number of bound states increases (see Fig. 6 for a schematic illustration). In Fig. 7, we compare the analytical estimates with the full numerical solution of Eqs. (15), for both the soliton and the qutrit wavefunctions, under experimentally feasible conditions.

Hamiltonian.— The interaction Hamiltonian is given by

$$H_{\text{int}} = g_{12} \int dx \psi_2^\dagger \psi_1^\dagger \psi_1 \psi_2, \quad (21)$$

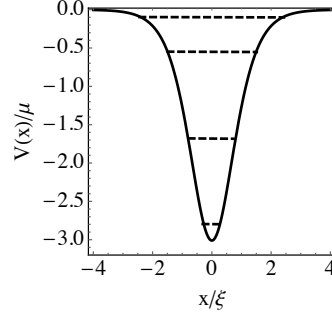


FIG. 6: (color online) Schematic representation of a four-level system obtained for $\nu = 10/7$. The upmost excited state exist at the border of the potential created by the dark soliton.

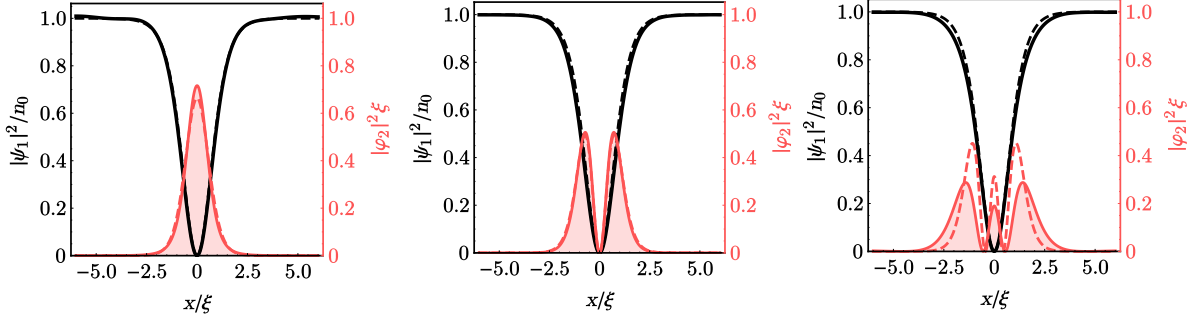


FIG. 7: (color online) Qutrits in a possible experimental situation: Numerical profiles of the dark soliton (black lines) and the impurity eigenstates (red lines). From left to right, we depict the ground state $\varphi_0(x)$, and the first and the second states, respectively $\varphi_1(x)$ and $\varphi_2(x)$, of a fermionic ^{133}Cs impurity trapped in a ^{85}Rb BEC dark soliton. The solid lines are the numerical solutions, while the dashed lines are the analytical expression described in the main text. We have used the following parameters: $m_2 = 1.56m_1$, $g_{12} = 1.25g_{11}$ (corresponding to $\nu = 1.13$). We fix the number of depleted condensate atoms by the dark soliton to be $n_0\xi \simeq 50$.

where $\psi_2(x) = \sum_{l=0}^2 \varphi_l(x) a_l$ describes the qutrit field in terms of the bosonic operators a_n , with $\varphi_0(x) = A_0 \text{sech}^\alpha(x/\xi)$, $\varphi_1(x) = 2A_1 \tanh(x/\xi) \varphi_0(x)$ and $\varphi_2(x) = \sqrt{2}A_2 (1 - (1 + 3\alpha) \tanh^2(x/\xi)) \varphi_0(x)$, where A_j ($j = 0, 1, 2$) are the normalization constants, given by

$$\begin{aligned}
 A_0 &= \left(\frac{\sqrt{\pi} \Gamma[\alpha]}{\Gamma[\frac{1+2\alpha}{2}]} \right)^{-\frac{1}{2}}, \\
 A_1 &= \left(2^{2(1+\alpha)} A_0^2 \left(\frac{{}_2F_1[\alpha, 2(1+\alpha), 1+\alpha, -1]}{\alpha} - \frac{{}_2F_1[1+\alpha, 2(1+\alpha), 2+\alpha, -1]}{1+\alpha} \right. \right. \\
 &\quad \left. \left. + \frac{{}_2F_1[2+\alpha, 2(1+\alpha), 3+\alpha, -1]}{2+\alpha} \right) \right)^{-\frac{1}{2}}, \\
 A_2 &= \left(2^{3+2\alpha} A_0^2 A_1^2 \left(\alpha {}_2F_1[\alpha, 2(2+\alpha), 1+\alpha, -1] - \frac{4\alpha(1+\alpha) {}_2F_1[1+\alpha, 2(2+\alpha), 2+\alpha, -1]}{1+\alpha} \right. \right. \\
 &\quad \left. \left. + \frac{(4+6\alpha^2+8\alpha) {}_2F_1[2+\alpha, 2(2+\alpha), 3+\alpha, -1]}{2+\alpha} - \frac{4\alpha(1\alpha) {}_2F_1[3+\alpha, 2(2+\alpha), 4+\alpha, -1]}{3+\alpha} \right. \right. \\
 &\quad \left. \left. + \frac{\alpha {}_2F_1[4+\alpha, 2(2+\alpha), 5+\alpha, -1]}{4+\alpha} \right) \right)^{-\frac{1}{2}}, \tag{22}
 \end{aligned}$$

where $\Gamma[\alpha]$ and ${}_2F_1$ represents the Gamma and Hypergeometric function, respectively, and $\alpha = \sqrt{2g_{12}m_2/g_{11}m_1}$. The inclusion of quantum fluctuations is performed by writing the BEC field as $\psi_1(x) = \psi_{\text{sol}}(x) + \delta\psi(x)$, where $\delta\psi(x) = \sum_k (u_k(x)b_k + v_k^*(x)b_k^\dagger)$ and b_k are the bosonic operators verifying the commutation relation $[b_k, b_q^\dagger] = \delta_{k,q}$. The amplitudes $u_k(x)$ and $v_k(x)$ satisfy the normalization condition $|u_k(x)|^2 - |v_k(x)|^2 = 1$ and are explicitly given

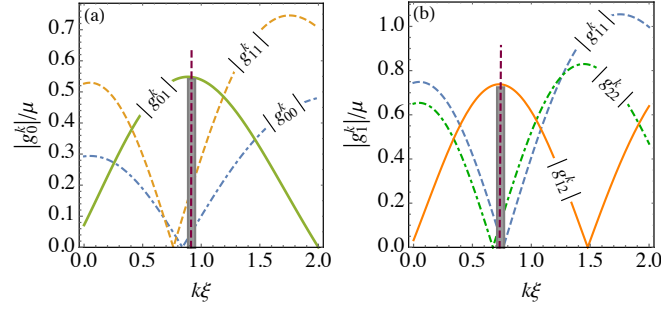


FIG. 8: (color online) Interband g_{il}^k ($l \neq l'$) (solid lines) and intraband g_{il}^k ($l = l'$) (dashed or dotted-dashed lines) coupling amplitudes. Near resonance, ($k \sim 0.9\xi^{-1}$ for the first transition, and $k \sim 0.7\xi^{-1}$ for the second transition), the interband terms clearly dominate over the intraband transitions, allowing us to neglect the latter within the rotating wave approximation.

by [4],

$$u_k(x) = \sqrt{\frac{1}{4\pi\xi} \frac{\mu}{\epsilon_k}} \times \left[\left((k\xi)^2 + \frac{2\epsilon_k}{\mu} \right) \left(\frac{k\xi}{2} + i \tanh\left(\frac{x}{\xi}\right) \right) + \frac{k\xi}{\cosh^2\left(\frac{x}{\xi}\right)} \right],$$

and

$$v_k(x) = \sqrt{\frac{1}{4\pi\xi} \frac{\mu}{\epsilon_k}} \times \left[\left((k\xi)^2 - \frac{2\epsilon_k}{\mu} \right) \left(\frac{k\xi}{2} + i \tanh\left(\frac{x}{\xi}\right) \right) + \frac{k\xi}{\cosh^2\left(\frac{x}{\xi}\right)} \right]$$

Using the rotating wave approximation (RWA), the first order perturbed Hamiltonian can be written as

$$H_{\text{int}}^{(1)} = \sum_k (g_0^k \sigma_0^+ + g_1^k \sigma_1^+) b_k + (g_0^{k*} \sigma_0^- + g_1^{k*} \sigma_1^-) b_k^\dagger, \quad (23)$$

where $\sigma_{0,1}^+ = a_{e_1, e_2}^\dagger a_{g, e_1}$, $\sigma_{0,1}^- = a_{g, e_1}^\dagger a_{e_1, e_2}$ and the coupling constants $g_{il}^k = g_i^k$ ($i = 0, 1$) are explicitly given by

$$\begin{aligned} g_0^k &= \frac{ig_{12}k^2\xi^{3/2}}{80\epsilon_k} \sqrt{\frac{n_0\pi}{6}} (2\mu + 8k^2\mu\xi^2 + 15\epsilon_k) (-4 + k^2\xi^2) \operatorname{csch}\left(\frac{k\pi\xi}{2}\right), \\ g_1^k &= \frac{ig_{12}k^2\xi^{3/2}}{896\epsilon_k} \sqrt{\frac{n_0\pi}{15}} [28(2k^4\xi^4 - 35k^2\xi^2 + 68)\epsilon_k \\ &\quad + \mu(29k^6\xi^6 - 504k^4\xi^4 + 896k^2\xi^2 + 64)] \operatorname{csch}\left(\frac{k\pi\xi}{2}\right). \end{aligned} \quad (24)$$

Technically speaking, the RWA approximation here means neglecting the intraband terms in Eq. (23), whose amplitudes are given by the coefficients g_{il}^k , illustrated in Fig. 8. This is achieved if we assume that only resonant processes (i.e. phonons with wavenectors k such that their energies ω_k are in resonance with the transitions ω_0 and ω_1 , promoting excitation–deexcitation of the impurity inside the soliton) participate in the dynamics. As explained in the main text, and as we see below, the validity of our RWA approximation is verified *a posteriori*, holding if the corresponding spontaneous emission rates γ_i ($i = 0, 1$) are much smaller than the qutrit transition frequencies ω_i .

Wigner-Weisskopf spontaneous decay.— We employ the Wigner-Weisskopf theory to find the spontaneous decay rate of the states, by neglecting the effect of temperature and other external perturbations. This is extremely well justified in our case, as BECs can nowadays be routinely produced well below the critical temperature for

condensations. The qutrit is assumed to be initially at the excited state $|e_2\rangle$ and the phonons to be in the vacuum state $|0\rangle$. Under such conditions, the wave function of total system (qutrit + phonons) can be described as

$$|\phi(t)\rangle = a(t) |e_2, 0\rangle + \sum_k b_k(t) |e_1, 1_k\rangle + \sum_{k,p} b_{k,p}(t) |g, 1_k, 1_p\rangle, \quad (25)$$

where $a(t)$ is the probability amplitude of the excited state $|e_2\rangle$. The qutrit decays to the state $|e_1\rangle$ with probability amplitude $b_k(t)$ by emitting a phonon of wavevector k and frequency ω_k . Subsequently, the qutrit de-excites to the ground state $|g\rangle$ via the emission of q -phonon of frequency ω_p and probability amplitude $b_{k,p}(t)$. The Wigner-Weisskopf ansatz (25) is then let to evolve under the total Hamiltonian in Eq. (23), for which the corresponding Schrödinger equation yields

$$\begin{aligned} \dot{a}(t) &= -\frac{\gamma_1}{2} a(t), \\ \dot{b}_k(t) &= -\frac{i}{\hbar} g_1^{k*} e^{i(\omega_k - \omega_1)t - \frac{\gamma_1}{2}t} - \frac{\gamma_0}{2} b_k(t), \\ \dot{b}_{k,p}(t) &= -\frac{i}{\hbar} g_0^{p*} b_k(t) e^{i(\omega_p - \omega_0)t}, \end{aligned} \quad (26)$$

which are simplified by following the procedure of Ref. [2]. Here, γ_i ($i = 0, 1$) is the i th state decay rate given by

$$\gamma_i = \frac{L}{\sqrt{2}\hbar\xi} \int d\omega_k \frac{\sqrt{1 + \eta_i}}{\eta_i} |g_i^k|^2 \delta(\omega_k - \omega_i), \quad (27)$$

with

$$\begin{aligned} \gamma_0 &= \frac{\pi N_0 g_{12}^2}{76800 \hbar \mu^5 \xi^2 \eta_0 \sqrt{\frac{\mu + \eta_0}{\mu}}} (-\mu + \eta_0) (-5\mu + \eta_0)^2 \\ &\times \left(8\eta_0 + 3\mu \left(-2 + 5\xi \sqrt{\frac{\hbar^2 \omega_0^2}{\mu^2 \xi^2}} \right) \right)^2 \text{csch}^2 \left(\frac{\pi \sqrt{-\mu + \eta_0}}{2\sqrt{\mu}} \right), \end{aligned} \quad (28)$$

and

$$\begin{aligned} \gamma_1 &= \frac{\pi N_0 g_{12}^2}{2.4 \times 10^7 \hbar \mu^7 \xi^2 \eta_1 \sqrt{\frac{\mu + \eta_1}{\mu}}} (-\mu + \eta_1) \left[-1956\mu^3 + \hbar^2 \omega_1^2 \left[-591\mu + 56\sqrt{\eta_1^2 - \mu^2} + 29\eta_1 \right] \right. \\ &\left. + 4\mu^2 \left[505\eta_1 + 7\sqrt{\frac{\eta_1^2}{\mu^2} - 1} (107\mu - 39\eta_1) \right] \right]^2 \text{csch}^2 \left(\frac{\pi \sqrt{-\mu + \eta_1}}{2\sqrt{\mu}} \right), \end{aligned} \quad (29)$$

where $\eta_i = \sqrt{\mu^2 + \hbar^2 \omega_i^2}$. In the long time limit $t \gg \gamma_i$, Eq. (26) can be simplified to obtain

$$\begin{aligned} a(t) &= e^{-\gamma_1 t/2}, \\ b_k(t) &= -i g_0^k \frac{[e^{i(\omega_k - \omega_1)t - \gamma_1 t/2} - e^{-\gamma_0 t/2}]}{i(\omega_k - \omega_1) - \frac{\gamma_1 - \gamma_0}{2}}, \\ b_{k,p}(t) &= \frac{g_0^k g_1^k}{i(\omega_k - \omega_1) - \frac{\gamma_1 - \gamma_0}{2}} \left[\frac{e^{i(\omega_p - \omega_0)t - \gamma_0 t/2} - 1}{i(\omega_p - \omega_0) - \frac{\gamma_0}{2}} + \frac{1 - e^{i(\omega_k + \omega_p - \omega_{eg})t - \gamma_1 t/2}}{i(\omega_k + \omega_p - \omega_{eg}) - \frac{\gamma_1}{2}} \right], \end{aligned} \quad (30)$$

where $\omega_{eg} = \omega_0 + \omega_1$, leading to Eq. (7) of the manuscript.

Heisenberg's relation and propagation. – With the aim of studying a dilute array of qutrits affects the propagation of sound waves inside the condensate, we compute the equation of motion for a weak acoustic probe coupling the ground and the first excited state (i.e. driving the lower transition of the qutrits). This is done with the help of Heisenberg's relation

$$i\hbar \frac{\partial(\delta\Psi)}{\partial t} = [\hat{H}, \delta\Psi], \quad (31)$$

where $\hat{H} = H_q + H_p + H_{\text{drive}}$ denotes the total Hamiltonian and $\delta\Psi = \phi b_q e^{iqx} + \psi^* b_q^\dagger e^{-iqx}$ is the fluctuating field with the Bogoliubov coefficients ϕ and ψ . Noticing that the commutation relation with the driving Hamiltonian provides

$$[H_{\text{drive}}, \delta\Psi] = \frac{g_0^k}{2\hbar} \rho_{12}, \quad (32)$$

where $\Omega_p = g_0^k \delta\Psi / \hbar$, and proceeding similarly for the commutation with H_q and H_p , we obtain the following wave equation

$$\frac{\partial \Omega_p}{\partial t} + \frac{\omega_q}{q} \frac{\partial \Omega_p}{\partial x} = -\frac{i}{2\hbar^2} (g_0^k)^2 \rho_{12}, \quad (33)$$

corresponding to Eq. (12) of the main text. The quantum interference with the second transition, driven by the coupling field of intensity $\Omega_c \gg \Omega_p$, is contained in the coherence ρ_{12} appearing in the rhs of Eq. (33). The latter can be identified as the acoustic analogue of a dynamical susceptibility.

* Electronic address: muzzamalshaukat@gmail.com

† Electronic address: hugo.tercas@tecnico.ulisboa.pt

- [1] M. Hohmann, F. Kindermann, B. Ganger, T. Lausch, D. Mayer, F. Schmidt and A. Widera, EPJ Quantum Technology Phys. Rev. A **2**, 23 (2015).
 [2] M. I. Shaukat, E. V. Castro and H. Terças, Phys. Rev. A **95**, 053618 (2017).
 [3] J. Lekner, Am. J. Phys. **75**, 1151 (2007).
 [4] J. Dziarmaga, Phys. Rev. A **70**, 063616 (2004).
-